한국복합신소재구조학회 논문집 제3권, 제3호, 2012년 9월
J. Korean Soc. Adv. Comp. Struc. Vol. 3, No. 3, pp. 22-30, September 2012
ISSN 2093-5145

적층된 복합 및 샌드위치 판 구조의 자유진동 해석을 위한 EAS 고체 유한요소

박대용[1] · 노명현[2] · 이상열[3]

대림사업 기술연구소 특수교량팀 과장[1], 포항산업과학연구원 강구조연구소 에너지인프라본부 선임연구원[2],
안동대학교 토목공학과 조교수[3]

EAS Solid Element for Free Vibration Analysis of Laminated Composite and Sandwich Plate Structures

Park, Dae-Yong[1] · Noh, Myung-Hyun[2] · Lee, Sang-Youl[3]

[1]Manager, Bridge Engineering Team, Daelim cooperation, Susong-Dong, Jongno-Gu, Seoul 100-732, South Korea
[2]Sr. Researcher, Energy Infrastructure Research Department, Steel Structure Research Division, Research Institute of Industrial Science & Technology, POSCO Global R&D Center 180-1, Songdo-Dong, Yeonsu-Gu, Incheon 406-840, South Korea
[3]Assistant Professor, Department of Civil Engineering, Andong National University, 388 Songchon-dong, Andong, Kyoungsangbuk-do 760-749, South Korea

Abstract: This study deals with an enhanced assumed strain (EAS) three-dimensional element for free vibration analysis of laminated composite and sandwich structures. The three-dimensional finite element (FE) formulation based on the EAS method for composite structures shows excellence from the standpoints of computational efficiency, especially for distorted element shapes. Using the EAS FE formulation developed for this study, the effects of side-to-thickness ratios, aspect ratios and ply orientations on the natural frequency are studied and compared with the available elasticity solutions and other plate theories. The numerical results obtained are in good agreement with those reported by other investigators. The new approach works well for the numerical experiments tested, especially for complex structures such as sandwich plates with laminated composite faces.

Key Words: EAS three-dimensional finite element, free vibration, laminates, composite structures, sandwich plates

1. Introduction

The structural members made of laminated composite and sandwich materials has been increased significantly due to their merits such as low density, high stiffnesses and high strengths. Analytical and numerical methods for free vibration of composite structures have been studied previously by a host of investigators using a variety of approaches. Srinivas et al. (1970) carried out a flexural vibration analysis of rectangular plates using an analytical solution. Noor and Burton (1990) developed an exact three-dimensional solution for stress and free vibration analysis of multilayered composite plates. Kant and Swaminathan (2001) presented analytical solution for free vibration of laminated composite and sandwich plates based on a higher-order shear deformation theory (HSDT). These works, based on analytical approaches, have limited capabilities in dealing with complex problems, primarily due to their limitations in handling different loading and

주요어: EAS 3차원 유한요소, 자유진동, 적층구조, 복합신소재 구조, 샌드위치 판

Corresponding author: Lee, Sang-Youl
Department of Civil Engineering, Andong National University, 388 Songchon-dong, Andong, Kyoungsangbuk-do 760-749, South Korea
Tel: +82-54-820-5847, E-mail: lsy@andong.ac.kr

투고일: 2012년 7월 27일 / 수정일: 2012년 8월 17일 / 게재확정일: 2012년 8월 29일

boundary conditions in the analysis. In order to overcome the limitations, many studies have been carried out using the finite element method for the free vibration analysis of rectangular composite plates based on different plate theories (Wu et al., 2010; Matsunaga, 2000; Lee and Wooh, 2004; Nayak et al., 2002). In general, finite elements with four or eight nodes per element can describe easily and accurately the kinematic behavior of a rectangular composite plate. However, the elements should be insensitive against mesh distortion that frequently occurs due to modern mesh generation tools or during finite deformations. Additionally such elements should not lock in thin structures and thus be applicable to shell problems. It is known that the best overall performance can be achieved by the assumed strain method developed by Simo and Hughes (1986). Andelfinger and Ramm (1993) presented the enhanced assumed strain (EAS) elements for two-dimensional, three-dimensional, plate and shell structures and their equivalence to HR-elements. Braes (1998) studied EAS elements and locking in membrane problems. Korelc et al. (2010) developed an improved EAS brick element for finite deformation in finite elasticity and plasticity. Computations with the EAS element are free from the shear locking and can yield accurate results for distorted element shapes (Han et al., 2006).

All these works are limited, in that they can analyze only the structural members made of isotropic materials. Thus, this study developed an EAS solid element for free vibration analysis of laminated composite and sandwich structures made of anisotropic materials. In order to validate the EAS solid element developed in this study, we compare our results with those published by various investigators.

2. Theoretical formulation

2.1 Enhanced assumed strain field

The variational basis of the finite element method with enhanced assumed strain (EAS) fields is based on the principle of Hu-Washizu in the following:

$$\prod\nolimits_{\mathbf{HW}}(\mathbf{u},\boldsymbol{\varepsilon},\boldsymbol{\sigma}) = \int_V \left[\frac{1}{2}\boldsymbol{\varepsilon}^{\mathrm{T}}\mathbf{T}\mathbf{C}\mathbf{T}^{\mathrm{T}}\boldsymbol{\varepsilon} + \boldsymbol{\sigma}^{\mathrm{T}}(\boldsymbol{\varepsilon}^{\mathrm{c}} - \boldsymbol{\varepsilon})\right] dV + \prod\nolimits_{ext}(\mathbf{u}) \tag{1}$$

$$\prod\nolimits_{ext}(\mathbf{u}) = -\int_V \mathbf{u}^{\mathrm{T}}\overline{\mathbf{b}}\, dV - \int_{S_\sigma} \mathbf{u}^{\mathrm{T}}\overline{\mathbf{t}}\, dS - \int_{S_u} \mathbf{t}^{\mathrm{T}}(\mathbf{u}-\overline{\mathbf{u}})\, dS + \int_V \mathbf{u}^{\mathrm{T}}\rho\ddot{\mathbf{u}}\, dV \tag{2}$$

where displacement field $\mathbf{u}$, strains $\boldsymbol{\varepsilon}$, and stresses $\boldsymbol{\sigma}$ are the free variables, $\mathbf{C}$ stands for the material stiffness matrix. The symbol ρ is mass density, which is defined as the inertial force per unit acceleration per unit volume. Prescribed values are marked by an upper bar, namely body force $\overline{\mathbf{b}}$, surface traction $\overline{\mathbf{t}}$, and the boundary conditions $\overline{\mathbf{u}}$ for prescribed displacements. $\mathbf{T}$ is the transformation matrix that the stresses and strains on the material axis can be transformed to those of the structural axis.

Following the idea of Simo and Rifai (1990), the assumed strains in the finite element calculations can be now split into a compatible part $\boldsymbol{\varepsilon}^{\mathrm{c}}$ that satisfies the geometric field equations in the strong sense and an enhanced part $\tilde{\boldsymbol{\varepsilon}}$:

$$\boldsymbol{\varepsilon} = \boldsymbol{\varepsilon}^{\mathrm{c}} + \tilde{\boldsymbol{\varepsilon}} = \mathbf{B}\mathbf{u} + \mathbf{M}\boldsymbol{\alpha} \tag{3}$$

where $\mathbf{B}$ is the compatible strain-displacement relation matrix, $\mathbf{M}$ is the interpolation matrix for the enhanced assumed strain fields, and $\boldsymbol{\alpha}$ is the vector of the internal strain parameters corresponding to the enhanced strain.

By substituting Eq. (3) into Eq. (1) with three-field functional, we get

$$\prod\nolimits_{\mathbf{EAS}}(\mathbf{u},\tilde{\boldsymbol{\varepsilon}},\boldsymbol{\sigma}) = \int_V \left[\frac{1}{2}(\mathbf{B}\mathbf{u}+\tilde{\boldsymbol{\varepsilon}})\mathbf{T}\mathbf{C}\mathbf{T}^{\mathrm{T}}(\mathbf{B}\mathbf{u}+\tilde{\boldsymbol{\varepsilon}}) - \boldsymbol{\sigma}^{\mathrm{T}}\tilde{\boldsymbol{\varepsilon}}\right] dV - \int_V \mathbf{u}^{\mathrm{T}}\overline{\mathbf{b}}\, dV - \int_{S_\sigma} \mathbf{u}^{\mathrm{T}}\overline{\mathbf{t}}\, dS - \int_{S_u} \mathbf{t}^{\mathrm{T}}(\mathbf{u}-\overline{\mathbf{u}})\, dS + \int_V \mathbf{u}^{\mathrm{T}}\rho\ddot{\mathbf{u}}\, dV \tag{4}$$

The Euler equations for the stationarity of this functional Eq. (4), in which boundary condition, force term, and mass term is removed, are

$$\int_V \delta\mathbf{u}^{\mathrm{T}}\mathbf{B}^{\mathrm{T}}\left[\mathbf{T}\mathbf{C}\mathbf{T}^{\mathrm{T}}(\mathbf{B}\mathbf{u}+\tilde{\boldsymbol{\varepsilon}})\right] dV = 0 \tag{5}$$

$$\int_V \delta\boldsymbol{\sigma}^{\mathrm{T}}\tilde{\boldsymbol{\varepsilon}}\, dV = 0 \tag{6}$$

$$\int_V \delta\tilde{\boldsymbol{\varepsilon}}^{\mathrm{T}}\left[\mathbf{T}\mathbf{C}\mathbf{T}^{\mathrm{T}}(\mathbf{B}\mathbf{u}+\tilde{\boldsymbol{\varepsilon}}) - \boldsymbol{\sigma}\right] dV = 0 \tag{7}$$

The enhanced assumed strain, defined in the global coordinate, is interpolated according to Eq. (3):

$$\tilde{\boldsymbol{\varepsilon}} = \mathbf{M}\boldsymbol{\alpha} \tag{8}$$

$$\mathbf{M} = \frac{\det \mathbf{J_0}}{\det \mathbf{J}} \mathbf{T_0^{-T}} \mathbf{M}_{\xi} \tag{9}$$

where $\det \mathbf{J}$ denotes the determinant of the Jacobian matrix $\mathbf{J}$, $\det \mathbf{J_0}$ is the determinant of the Jacobian matrix $\mathbf{J_0} = \mathbf{J}|_{\xi=\eta=\zeta=0}$ at center($\xi=\eta=\zeta=0$) of the elementinthe natural coordinate, and $\mathbf{M}_{\xi}$ is the shape or interpolation function for the enhanced assumed strain, respectively. According to tensor calculus, $\mathbf{T_0^{-T}}$ maps the polynomial shape functions of $\mathbf{M}_{\xi}$, defined in the natural coordinate, into the global coordinate (Simo and Rafai, 1990).

This transformation is restricted to the origin so that the components of $\mathbf{T_0^{-T}}$ are constant and the chosen polynomial order is not increased. Then the matrix $\mathbf{T_0^{-T}}$ contains the components J_{ij_0} of $\mathbf{J_0}$ and can be written as $\mathbf{J_0}$ where are the components of Jacobian matrix J_{ij_0} at the center of the element in the natural coordinate. The Jacobian matrix at the center of the element ($\xi=\eta=\zeta=0$) does not originate the unexpected strain energy by the enhanced strain. The revised Jacobian at center of element then guarantees that the patch test is passed.

In Eq. (9), $\mathbf{M}_{\xi}$ must be assumed by the linear independent interpolation functions that satisfy the orthogonality of Eq. (6) (Simo and Rifai, 1990). Therefore, an optimal interpolation of $\mathbf{M}_{\xi}$ for the enhanced assumed strain can be found by inspecting the polynomial field of the compatible strain in the natural coordinate system. In order to decouple and enhance compatible strains, following complete trilinear 30-parameters interpolation function in the natural coordinate was chosen (Andelfinger and Ramm, 1993):

$$\mathbf{T_0} = \begin{bmatrix} J_{11_0}^2 & J_{21_0}^2 & J_{31_0}^2 & 2J_{11_0}J_{21_0} & 2J_{21_0}J_{31_0} & 2J_{11_0}J_{31_0} \\ J_{12_0}^2 & J_{22_0}^2 & J_{32_0}^2 & 2J_{12_0}J_{22_0} & 2J_{22_0}J_{32_0} & 2J_{12_0}J_{32_0} \\ J_{13_0}^2 & J_{23_0}^2 & J_{33_0}^2 & 2J_{13_0}J_{23_0} & 2J_{23_0}J_{33_0} & 2J_{13_0}J_{33_0} \\ J_{11_0}J_{12_0} & J_{21_0}J_{22_0} & J_{31_0}J_{32_0} & J_{11_0}J_{22_0}+J_{21_0}J_{12_0} & J_{21_0}J_{32_0}+J_{31_0}J_{22_0} & J_{11_0}J_{32_0}+J_{31_0}J_{12_0} \\ J_{12_0}J_{13_0} & J_{22_0}J_{23_0} & J_{32_0}J_{33_0} & J_{12_0}J_{23_0}+J_{22_0}J_{13_0} & J_{22_0}J_{33_0}+J_{32_0}J_{23_0} & J_{12_0}J_{33_0}+J_{32_0}J_{13_0} \\ J_{11_0}J_{13_0} & J_{21_0}J_{23_0} & J_{31_0}J_{33_0} & J_{11_0}J_{23_0}+J_{21_0}J_{13_0} & J_{21_0}J_{33_0}+J_{31_0}J_{23_0} & J_{11_0}J_{33_0}+J_{31_0}J_{13_0} \end{bmatrix} \tag{10}$$

$$\mathbf{M}_{\xi} = \left[\begin{array}{ccc|cccccc|cccccc} \xi & 0 & 0 & 0 & 0 & 0 & 0 & 0 & 0 & 0 & 0 & 0 & 0 & 0 & 0 \\ 0 & \eta & 0 & 0 & 0 & 0 & 0 & 0 & 0 & 0 & 0 & 0 & 0 & 0 & 0 \\ 0 & 0 & \zeta & 0 & 0 & 0 & 0 & 0 & 0 & 0 & 0 & 0 & 0 & 0 & 0 \\ 0 & 0 & 0 & \xi & \eta & 0 & 0 & 0 & 0 & \xi\zeta & \eta\zeta & 0 & 0 & 0 & 0 \\ 0 & 0 & 0 & 0 & 0 & \eta & \zeta & 0 & 0 & 0 & 0 & \xi\eta & \xi\zeta & 0 & 0 \\ 0 & 0 & 0 & 0 & 0 & 0 & 0 & \xi & \zeta & 0 & 0 & 0 & 0 & \xi\eta & \eta\zeta \end{array}\right.$$

$$\left.\begin{array}{cccccc|ccc|ccc|ccc} \xi\eta & \xi\zeta & 0 & 0 & 0 & 0 & 0 & 0 & 0 & \xi\eta\zeta & 0 & 0 & 0 & 0 & 0 \\ 0 & 0 & \xi\eta & \eta\zeta & 0 & 0 & 0 & 0 & 0 & 0 & \xi\eta\zeta & 0 & 0 & 0 & 0 \\ 0 & 0 & 0 & 0 & \xi\zeta & \eta\zeta & 0 & 0 & 0 & 0 & 0 & \xi\eta\zeta & 0 & 0 & 0 \\ 0 & 0 & 0 & 0 & 0 & 0 & \xi\eta & 0 & 0 & 0 & 0 & 0 & \xi\eta\zeta & 0 & 0 \\ 0 & 0 & 0 & 0 & 0 & 0 & 0 & \eta\zeta & 0 & 0 & 0 & 0 & 0 & \xi\eta\zeta & 0 \\ 0 & 0 & 0 & 0 & 0 & 0 & 0 & 0 & \xi\zeta & 0 & 0 & 0 & 0 & 0 & \xi\eta\zeta \end{array}\right] \tag{11}$$

2.2 Finite element formulation

Eqs. (8) and (9) are introduced into the energy principle of Eq. (4), and variation with respect to the unknown parameters $\mathbf{d_i}$ and $\boldsymbol{\alpha}_i$ results in the following system of equations:

$$\begin{bmatrix} \mathbf{K_{CC}} & \mathbf{K_{CN}} \\ \mathbf{K_{CN}^T} & \mathbf{K_{NN}} \end{bmatrix}^e \begin{bmatrix} \mathbf{d_i} \\ \boldsymbol{\alpha}_\mathbf{i} \end{bmatrix}^e = \begin{bmatrix} \mathbf{F} \\ \mathbf{0} \end{bmatrix}^e \tag{12}$$

where $\mathbf{F}$ is the vector of applied nodal forces used in the displacement method, $\mathbf{d_i}$ is the nodal displacements of node i in the global coordinate system, and the stiffness matrix $\mathbf{K_{CC}}$, $\mathbf{K_{CN}}$, $\mathbf{K_{NN}}$ are described as

$$\begin{aligned} \mathbf{K_{CC}} &= \int_V \mathbf{B^T Q B}\, dV \\ &= \sum_{l=1}^{n}\sum_{k=1}^{n}\sum_{j=1}^{n} R_j R_k R_l\, \mathbf{B^T Q B} \left|\mathbf{J}(\xi_j, \eta_k, \zeta_l)\right| \end{aligned} \tag{13}$$

$$\begin{aligned} \mathbf{K_{CN}} &= \int_V \mathbf{B^T Q M}\, dV \\ &= \sum_{l=1}^{n}\sum_{k=1}^{n}\sum_{j=1}^{n} R_j R_k R_l\, \mathbf{B^T Q M} \left|\mathbf{J}(\xi_j, \eta_k, \zeta_l)\right| \end{aligned} \tag{14}$$

$$\begin{aligned} \mathbf{K_{NN}} &= \int_V \mathbf{M^T Q M}\, dV \\ &= \sum_{l=1}^{n}\sum_{k=1}^{n}\sum_{j=1}^{n} R_j R_k R_l\, \mathbf{M^T Q M} \left|\mathbf{J}(\xi_j, \eta_k, \zeta_l)\right| \end{aligned} \tag{15}$$

where n is the number of Gauss points, and Q is the material stiffness matrix as following:

$$\mathbf{Q} = \mathbf{TCT^T} \tag{16}$$

where C is the material stiffness matrix as Eq. (17).

$$\mathbf{C} = \begin{bmatrix} 1/E_x & -\nu_{yx}E_y & -\nu_{zx}E_z & 0 & 0 & 0 \\ -\nu_{xy}/E_x & 1/E_y & -\nu_{zy}/E_z & 0 & 0 & 0 \\ -\nu_{xz}/E_x & -\nu_{yz}/E_y & 1/E_z & 0 & 0 & 0 \\ 0 & 0 & 0 & 1/G_{xy} & 0 & 0 \\ 0 & 0 & 0 & 0 & 1/G_{yz} & 0 \\ 0 & 0 & 0 & 0 & 0 & 1/G_{xz} \end{bmatrix}^{-1} \tag{17}$$

The stress-strain for the structural axis is obtained by

$$\boldsymbol{\sigma}_s = \mathbf{T}\boldsymbol{\sigma}_m = \mathbf{T}\mathbf{C}\boldsymbol{\varepsilon}_m = \mathbf{T}\mathbf{C}\mathbf{T}^T\boldsymbol{\varepsilon}_s \tag{18}$$

Fig. 1 shows the relationship between the structural or problem axis ($1-2-3$) and the material axis ($x-y-z$) for a lamina. Finally the stress-strain relations for an orthotropic material in the structural axis can be also expressed as

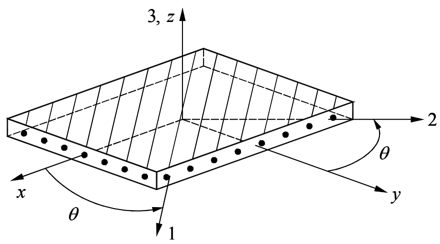

Fig. 1 A fiber-reinforced lamina with structure ($x-y-z$) and material ($1-2-3$) coordinate system ($+\theta$: counterclockwise).

$$\boldsymbol{\sigma}_s = \begin{bmatrix} \sigma_{xx} \\ \sigma_{yy} \\ \sigma_{zz} \\ \sigma_{xy} \\ \sigma_{yz} \\ \sigma_{zx} \end{bmatrix} = \begin{bmatrix} Q_{11} & Q_{12} & Q_{13} & Q_{14} & 0 & 0 \\ Q_{12} & Q_{22} & Q_{23} & Q_{24} & 0 & 0 \\ Q_{13} & Q_{23} & Q_{33} & Q_{34} & 0 & 0 \\ Q_{14} & Q_{24} & Q_{34} & Q_{44} & 0 & 0 \\ 0 & 0 & 0 & 0 & Q_{55} & Q_{56} \\ 0 & 0 & 0 & 0 & Q_{56} & Q_{66} \end{bmatrix} \begin{bmatrix} \varepsilon_{xx} \\ \varepsilon_{yy} \\ \varepsilon_{zz} \\ \varepsilon_{xy} \\ \varepsilon_{yz} \\ \varepsilon_{zx} \end{bmatrix} = \mathbf{Q}\boldsymbol{\varepsilon}_s \tag{19}$$

Here, $\boldsymbol{\alpha}_i$ must be removed from Eq.(12), because it is an artificial parameter used for an enhanced strain. Then the static condensation for the strain parameter $\boldsymbol{\alpha}_i$ finally yields the element stiffness matrix as following:

$$\mathbf{K}^e = \mathbf{K}_{CC} - \mathbf{K}_{CN}\mathbf{K}_{NN}^{-1}\mathbf{K}_{CN}^T \tag{20}$$

In this study, the finite element obtained by these procedures is named by "EAS-SOLID8".

Assuming uniform distribution of mass whose density is ρ, measured per unit volume, the consistent element mass matrix $\mathbf{M}^e$ in terms of nodal displacements, $\mathbf{u} = \begin{bmatrix} u & v & w \end{bmatrix}^T$, is

$$\mathbf{M}^e = \int_V \mathbf{N}^T \rho \mathbf{N}\, dV = \sum_{l=1}^{n}\sum_{k=1}^{n}\sum_{j=1}^{n} R_j R_k R_l \mathbf{N}_{jkl}^T \rho \mathbf{N}_{jkl} \left|\mathbf{J}_{jkl}\right| \tag{21}$$

In Eq. (21), N is the shape function matrix and the matrix $\left|\mathbf{J}_{jkl}\right|$ and $\mathbf{N}_{jkl}$ are evaluated at each intergration point $\left(\xi_j, \eta_k, \zeta_l\right)$ $\mathbf{N}$. The shape function matrix can be written as

$$\mathbf{N}_{[3\times24]} = \begin{bmatrix} N_1 & 0 & 0 & N_2 & & & \cdots & N_8 \\ & N_1 & 0 & 0 & N_2 & & \cdots & N_8 \\ & & N_1 & 0 & 0 & N_2 & \cdots & N_8 \end{bmatrix} \tag{22}$$

where,

$$\mathrm{N}_i = \frac{1}{8}\left(1+\xi\xi_i\right)\left(1+\eta\eta_i\right)\left(1+\zeta\zeta_i\right) \text{ and}$$
$$i = 1,....,8,\ \xi_i, \eta_i, \zeta_i = \pm 1$$

The basic equation of vibration analysis of undamped system in the form of an eigen problem is

$$\left(\mathbf{K}^e - \omega^2\mathbf{M}^e\right)\mathbf{d} = 0 \tag{23}$$

where ω is the fundamental frequencies, $\mathbf{d}$ is the displacement vector.

3. Numerical examples

The finite element formulation described earlier is now implemented to compare the results of our technique with those published by other investigators and also to study the influences on the analysis of two or three-dimensional composite structures. Fig. 2 shows the dimensions of a simply supported composite plate analyzed by the aforementioned formulations for the materials whose properties are listed in Table 1.

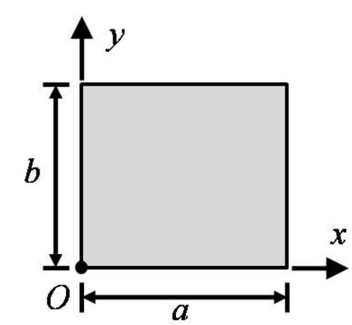

Fig. 2 Dimensions of a simply supported composite plate

Note that the properties of Materials I, II and III are normalized by E2. The units of E1, E2, G12, G23, G13 are GPa and that of ρ is kg/m3, respectively.

3.1 Cross-ply

Table 2 shows natural frequencies of an antisymmetric cross-ply square laminated plates with a/h=5.0 and a/b=1.0. The sides of the plate made of Material I are simply supported and the natural frequencies are normalized as $\bar{\omega}=\left(\omega\times b^2/h\right)\sqrt{\rho/E_2}$. The mesh divisions of 4x4 or 8x8 or 10x10 for a quarter plate model are applied for different number of layers (2, 4, 8, and 10) and E1/E2 ratios. From 8x8 mesh division, the numerical results obtained from this study using EAS-SOLID8 are in good agreement with those reported by other investigators.

In order to validate the FEM code developed for different side-to-thickness ratios, the natural frequency of a symmetric cross-ply composite laminate made of Material II is computed and compared with various results reported by other investigators. Table 3 shows non-dimensionalized fundamental frequencies of a simply supported symmetric cross-ply square laminated plates for different side-to-thickness ratios. It can be observed from the table that present results are in very good agreement with analytical solutions of Kant-Swaminathan regardless of side-to-thickness ratios. It is known in general that for thin plates a somewhat difference exists between the results obtained from solid and 2-D models (Noh et al., 2012). On the other s hand, the frequencies obtained by the EAS-SOLID8 give better accurate because of the significant influences of the enhanced assumed strain.

3.2 Angle-ply

Non-dimensionalized natural frequencies of simply supported anti-symmetric angle-ply square laminated plates with different fiber angles and thickness-length ratios (h/a). The material properties of the individual layers of plates are given by Material III and the induced natural frequencies are normalized as $\bar{\omega}=\left(\omega\times b^2/h\right)\sqrt{\rho/E_2}$. Note that a two-dimensional exact solution are used by Noor-Burton and Xiaoping, while a 12X12 mesh of EAS three-dimensional elements is used in this study.

Table 4 represents Non-dimensionalized natural frequencies of a simply supported anti-symmetric angle-ply square laminated plates with h/a made of Material III. The natural frequencies obtained by the EAS three-dimensional element are mostly higher than those by two-dimensional solution. The differences between two and three-dimensional formulations depend on many parameters such as ply angles, number of layers, length-to-thickness ratio, and boundary conditions.

Table 5 shows natural frequencies for a simply supported $[45/-45]_4$ square laminated plates with a/h. The present model is also compared with the classical plate theory (CPT), the uniform shear deformational theory with shear correction factor 5/6 (USDT) and the parabolic shear deformation theory (PSDT) in predicting the natural frequencies of composite plates made of Material II. It is observed from the table that the results of USDT, PSDT, and Xiaoping theory are in good agreement with those produced by present model regardless of thickness-length ratios.

3.3 Five-layer sandwich plate

Figs 3~4 show natural frequencies of a simply supported sandwich plate with anti-symmetric cross-ply face sheets for different side-to-thickness ratios(a/h) and aspect ratios(a/b). The material properties of the individual layers of plates are given by Material III and the induced natural frequencies are normalized as $\bar{\omega}=\left(\omega\times b^2/h\right)\sqrt{\rho/E_2}$. y

Table 1. Mechanical and physical properties of the materials used in this study

Material		E_1	E_2	E_3	G_{12}	G_{13}	G_{23}	ν_{12}	ν_{13}	ν_{23}	ρ
Material I		open	-	E_2	0.6 E_2	0.6 E_2	0.5 E_2	0.25	0.25	0.25	1.0
Material II		40 E_2	-	E_2	0.6 E_2	0.6 E_2	0.5 E_2	0.25	0.25	0.25	1.0
Material III		15 E_2	-	E_2	0.6 E_2	0.5 E_2	0.5 E_2	0.30	0.30	0.49	1.0
Material IV (Sandwich)	Core	131	10.34	10.34	6.895	6.205	6.895	0.22	0.22	0.49	1627
	Face	0.00689	0.00689	0.00689	0.00345	0.00345	0.00345	0	0	0	97

Table 2. Nondimensionalized fundamental frequencies for a simply supported antisym metric cross-ply square laminated plates with a/h=5, a/b=1.0.

Lamination and numberof layers	Source	MESH	E_1/E_2				
			3	10	20	30	40
$[0/90]_1$	Present study (EAS-SOLID8)	4X4	6.3846	7.1351	7.8641	8.4070	8.8325
		8X8	6.3159	7.0576	7.7803	8.3201	8.7440
		10X10	6.3078	7.0484	7.7704	8.3097	8.7335
	3D Elasticity(Noor, 1973)	Exact	6.2578	6.9845	7.6745	8.1763	8.5625
	Rao et al.(2004)-a	Refined	6.2317	6.9555	7.6427	8.1423	8.5269
	Rao et al.(2004)-b	ESL	6.2336	6.9740	7.7138	8.2770	8.7266
	Kant-Swaminathan(2001)-a	HSDT	6.2336	6.9741	7.7140	8.2775	8.7272
	Kant-Swaminathan(2001)-b	HSDT	6.1566	6.9363	7.6883	8.2570	8.7097
	Reddy(1984)	HSDT	6.2169	6.9887	7.8210	8.5050	9.0871
	Senthilnathan et al.(1987)	HSDT	6.2169	6.9887	7.8210	8.5050	9.0871
	Whitney-Pagano(1970)	FSDT	6.1490	6.9156	7.6922	8.3112	8.8255
$[0/90]_2$	Present study (EAS-SOLID8)	4X4	6.6234	8.2789	9.6040	10.4100	10.9587
		8X8	6.5525	8.1927	9.5116	10.3166	10.8659
		10X10	6.5440	8.1824	9.5006	10.3055	10.8549
	3D Elasticity(Noor, 1973)	Exact	6.5455	8.1445	9.4055	10.1650	10.6798
	Rao et al.(2004)-a	Refined	6.5044	8.0928	9.3453	10.0998	10.6111
	Rao et al.(2004)-b	ESL	6.5145	8.1483	9.4675	10.2731	10.8219
	Kant-Swaminathan(2001)-a	HSDT	6.5146	8.1482	9.4675	10.2733	10.8221
	Kant-Swaminathan(2001)-b	HSDT	6.4319	8.1010	9.4338	10.2463	10.7993
	Reddy(1984)	HSDT	6.5008	8.1954	9.6265	10.5348	11.1716
	Senthilnathan et al.(1987)	HSDT	6.5008	8.1954	9.6265	10.5348	11.1716
	Whitney-Pagano(1970)	FSDT	6.4402	8.1963	9.6729	10.6095	11.2635
$[0/90]_3$	Present study (EAS-SOLID8)	4X4	6.6706	8.5092	9.9676	10.8461	11.4394
		8X8	6.5992	8.4205	9.8718	10.7491	11.3431
		10X10	6.5907	8.4099	9.8604	10.7376	11.3315
	3D Elasticity(Noor, 1973)	Exact	6.6100	8.4143	9.8398	10.6958	11.2728
	Rao et al.(2004)-a	Refined	6.5638	8.3549	9.7695	10.6190	11.1918
	Rao et al.(2004)-b	ESL	6.5712	8.3858	9.8353	10.7117	11.3052
	Kant-Swaminathan(2001)-a	HSDT	6.5711	8.3852	9.8346	10.7113	11.3051
	Kant-Swaminathan(2001)-b	HSDT	6.4873	8.3372	9.8012	10.6853	11.2838
	Reddy(1984)	HSDT	6.5552	0.4041	9.9175	10.8542	11.5007
	Senthilnathan et al.(1987)	HSDT	6.5552	0.4041	9.9175	10.8542	11.5007
	Whitney-Pagano(1970)	FSDT	6.4916	8.3883	9.9266	10.8723	11.5189
$[0/90]_5$	Present study (EAS-SOLID8)	4X4	6.6953	8.6309	10.1643	11.0883	11.7134
		8X8	6.6235	8.5407	10.0663	10.9888	11.6143
		10X10	6.6150	8.5300	10.0546	10.9769	11.6025
	3D Elasticity(Noor, 1973)	Exact	6.6458	8.5625	10.0843	11.0027	11.6245
	Rao et al.(2004)-a	Refined	6.5955	8.4970	10.0640	10.9173	11.5341
	Rao et al.(2004)-b	ESL	6.6019	8.5164	10.0440	10.9698	11.5992
	Kant-Swaminathan(2001)-a	HSDT	6.6019	8.5163	10.0438	10.9699	11.5993
	Kant-Swaminathan(2001)-b	HSDT	6.5177	8.4680	10.0107	10.9445	11.5789
	Reddy(1984)	HSDT	6.5842	8.5126	10.0674	11.0197	11.6730
	Senthilnathan et al.(1987)	HSDT	6.5842	8.5126	10.0674	11.0197	11.6730
	Whitney-Pagano(1970)	FSDT	6.5185	8.4842	10.0483	10.9959	11.6374

Table 3. Nondimensionalized fundamental frequencies of a simply supported symmetric cross-ply square laminated plates for different side-to-thickness ratios.

	Source		Side-to-thickness ratio (*a/h*)					
			2	4	10	20	50	100
[0/90]	EAS-SOLID8	4X4	5.1544	7.9926	10.6005	11.2642	11.4765	11.5080
		8X8	5.1197	7.9200	10.4698	11.1141	11.3198	11.3503
		10X10	5.1155	7.9113	10.4543	11.0963	11.3013	11.3316
	Kant-Swaminathan(2001)[a]	HSDT	5.0918	7.9081	10.4319	11.0663	11.2688	11.2988
	Kant-Swaminathan(2001)[b]	HSDT	5.0746	7.8904	10.4156	11.0509	11.2537	11.2837
	Reddy(1984)	HSDT	5.7170	8.3546	10.5680	11.1052	11.2751	11.3002
	Senthilnathan et al.(1987)	HSDT	5.7170	8.3546	10.5680	11.1052	11.2751	11.3002
	Whitney-Pagano(1970)	FSDT	5.2085	8.0889	10.4610	11.0639	11.2558	11.2842
[0/90/90/0]	EAS-SOLID8	4X4	5.5000	9.4925	15.3122	18.0061	19.0338	19.1975
		8X8	5.4669	9.4213	15.0568	17.7724	18.7685	18.9270
		10X10	5.4629	9.4127	15.0018	17.7446	18.7371	18.8949
	Kant-Swaminathan(2001)[a]	HSDT	5.4033	9.2870	15.1048	17.6470	18.6720	18.8357
	Kant-Swaminathan(2001)[b]	HSDT	5.3929	9.2710	15.0949	17.6434	18.6713	18.8355
	Reddy(1984)	HSDT	5.5065	9.3235	15.1073	17.6457	18.6718	18.8356
	Senthilnathan et al.(1987)	HSDT	6.0017	10.2032	15.9405	17.9938	18.7381	18.8526
	Whitney-Pagano(1970)	FSDT	5.4998	9.3949	15.1426	17.6596	18.6742	18.8362

Table 4. Nondimensionalized natural frequencies of a simply supported anti-symmetric [Θ/-Θ/⋯⋯] angle-ply square laminated plates with h/a (Material III).

Lay-up	Source	MESH	*h/a*			
			0.01	0.1	0.2	0.3
$[15/-15]_5$	EAS-SOLID8	8X8	0.001360	0.1193	0.3708	0.6564
		10X10	0.001353	0.1187	0.3693	0.6540
		12X12	0.001349	0.1184	0.3685	0.6528
	Noor-Burton(1990)	Exact	0.001328	0.1162	0.3588	0.6307
	Xiaoping(2001)		0.001328	0.1160	0.3577	0.6280
$[30/-30]_5$	EAS-SOLID8	8X8	0.001537	0.1337	0.4100	0.7155
		10X10	0.001531	0.1331	0.4085	0.7130
		12X12	0.001527	0.1328	0.4076	0.7117
	Noor-Burton(1990)	Exact	0.001510	0.1296	0.3889	0.6692
	Xiaoping(2001)		0.001510	0.1294	0.3880	0.6676
$[45/-45]_5$	EAS-SOLID8	8X8	0.001619	0.1400	0.4260	0.7392
		10X10	0.001613	0.1394	0.4244	0.7367
		12X12	0.001610	0.1391	0.4235	0.7353
	Noor-Burton(1990)	Exact	0.001595	0.1351	0.3993	0.6810
	Xiaoping(2001)		0.001595	0.1350	0.3987	0.6804

Table 5. Nondimensionalized natural frequencies for a simply supported [45/-45]4square laminated plates with a/h (Material II).

Lay-up	Source	MESH	*h/a*			
			0.01	0.1	0.2	0.25
$[45/-45]_4$	EAS-SOLID8	8x8	25.563	18.8069	12.3662	10.3966
		10x10	25.490	18.7271	12.3209	10.3605
		12x12	25.447	18.6810	12.2958	10.3405
	CPT		25.264	25.0520	15.7080	12.5660
	USDT		25.176	19.2890	12.8920	10.8420
	PSDT		25.174	19.2660	12.9720	10.9910
	Xiaoping(2001)		25.169	19.0200	12.6440	10.6360

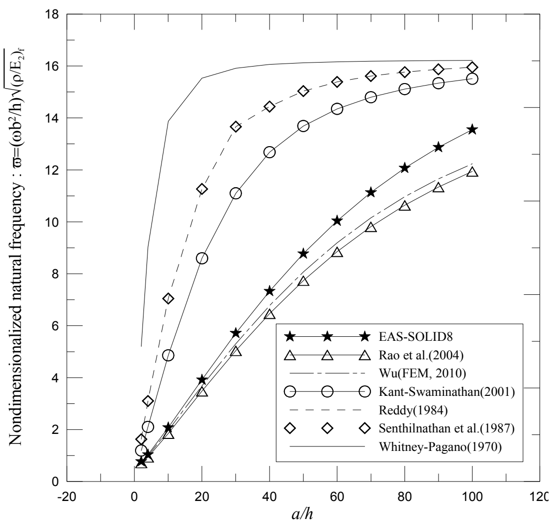

Fig. 3 Non-dimensionalized natural frequency versus side-to-thicknessratio (a/h) of a simply supported five-layer sandwich plate with antisymmetric cross-ply face sheets

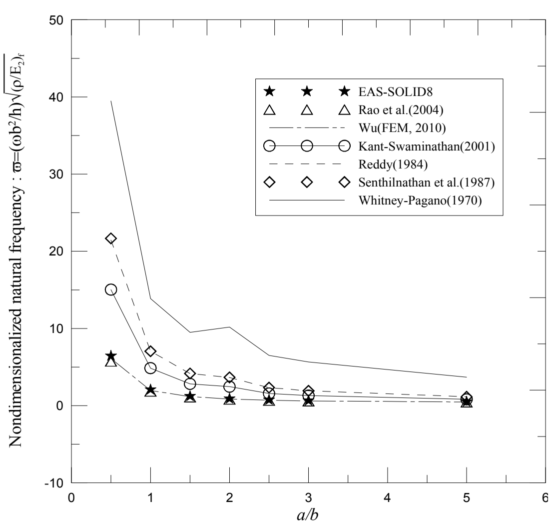

Fig. 4 Non-dimensionalized natural frequency versus aspect ratio (a/b) of a simply supported five-layer sandwich plate with antisymmetric cross-ply face sheets

It is observed from the figures that the recent results of Rao et al.(2004) and Wu (2010) are in good agreement with those produced by present model regardless of side-to-thickness and aspect ratios. On the other hand, the results of Senthilnanthan et al. (1987) and Kan-Swaminathan (2001) theories overestimate the natural frequencies for different side-to-thickness ratios and aspect ratios. In dealing with such complex sandwich types, it is critical to provide high computational efficiency and stable result. EAS-SOLID8 may make contributions to meet the demands.

4. Summary and conclusion

In this study, the solid finite element (EAS-SOLID8) with an enhanced assumed strain field is developed to further study free vibration of laminated composite and sandwich plates. The EAS-SOLID8, in comparison with another conventional element, is more attractive not only because it can analyze general thick plates but also it shows accurate results for thin structures. For laminated composite plates, the results by using the EAS-SOLID8 are observed to be in excellent agreement with the three-dimensional elasticity solutions and other finite element results. For sandwich plates, the recent results of Rao et al and Wu are in good agreement with those produced by the EAS-SOLID8 regardless of side-to-thickness and aspect ratios.

It is concluded from this study that the approach works well for the numerical experiments tested, especially for complex structures such as anisotropic plates. However, the examples might be too simplistic to extract conclusions for varies parameters. In order to prove the effectiveness of the technique, it will be necessary to prove the concept from more complicated parameters such as delamination problems.

감사의 글

이 논문은 2012년도 정부(교육과학기술부)의 재원으로 한국연구재단의 지원을 받아 수행된 기초연구사업임(No. 2012R1A1A1014722).

References

Andelfinger, U. and Ramm, E. (1993). “EAS-elements for two-dimensional three-dimensional, plate and shell structures and their equivalence to HR-elements.” *Int. J. Numer. Methods Eng.,* 36, pp.1311-1337.

Braes, D. (1998). “Enhanced assumed strain elements and locking in membrane problems.” *Comp. Meth. Appl. Mech. Engineering,* 165, pp.155-174.

Kant, T. and Swaminathan, K. (2001). “Analytical solutions for free vibration of laminated composite and sandwich plates based on a higher-order refined theory.” *Comp. Struct.,* 53, pp.73-85.

Kant, T. and Swaminathan, K. (2001). “Free vibration of isotropic, orthotropic, and multilayer plates based on higher order refined theories.” *J Sound Vib.,* 241, pp.319-27.

Han, S. C., Lee, S. Y., and Rus, G. (2010). “Postbuckling analysis of laminated composite plates subjected to the combination of in-plane shear, compression and lateral loading.” *Int. J. Solids Struct.,* 43, pp.5713-5735.

Korelc, J, Šolinc U., and Wriggers P. (2010). “An improved EAS brick element for finite deformation.” *Comp. Mech.,* 46, pp.641-659.

Lee, S. Y. and Wooh, S. C. (2004). “Finite element vibration analysis of composite box structures using the high order plate theory.” *J. Sound Vib.,* 277, pp.801-814.

Matsunaga, H. (2000). “Vibration and stability of cross-ply laminated composite plates according to a global higher-order plate theory.” *Compos. Struct,* 48, pp.231-44..

Nayak. A. K., Moy, S. S. J., and Shenoi, R. A. (2002). “Free vibration analysis of composite sandwich plates based on Reddy’s higher-order theory.” *Composites: Part B,* 33, pp.505-19.

Noh, Y. H., Park, D. Y., and Lee, S. Y. (2012). “Free vibration of three-dimensional laminated composite structures with different embedded delamination sizes and locations.” *J. Korean Soc. Adv. Comp. Struc.,* 3(1), pp.1-11.

Noor, A. K. (1973). “Free vibrations of multilayered composite plates.” *AIAA J,* 11, pp.1038-1039.

Noor, A. K. and Burton, W. S. (1990). “Three-dimensional solutions for antisymmetrically laminated anisotropic plates.” *J. Appl Mech,* 57, pp.183-8.

Pian, T. H. H. and Sumihara, K. (1984). “Rational approach for assumed stress finite elements.” *Int. J. Numer. Methods Eng.,* 20, pp.1685-1695.

Rao, M. K., Scherbatiuk, K., Desai, Y. M., and Shah, A. H. (2004). “Natural vibrations of laminated and sandwich plates.” *J Eng Mech.,* 130, pp.1268-1278.

Reddy, J. N. (1984). “simple higher order theory for laminated composite plates,” *ASME J. App. Mech.,* 51, pp.745-752.

Senthilnathan, N. R., Lim, K. H., Lee, K. H., and Chow, S. T. (1987). “Buckling of shear deformables plates,” *AIAA J.,* 25(9), pp.1268-1271.

Simo, J. C., Hughes, T. J. R. (1986). “On the variational formulations of assumed strain methods. Journal of Applied Mechanics,” *ASME,* 53, pp.51-54.

Simo, J.C. and Rifai, M.S. A (1990). “class of mixed assumed strain methods and the method of incompatible modes,” *Int. J. Numer. Methods Eng.,* 29, pp.1595-1638.

Srinivas, S., Joga Rao, C. V., and Rao, A. K. (1970). “An exact analysis for vibration of simply supported homogeneous and laminated thick rectangular plates.” *J. Sound Vib.,* 12(2), pp.187-199.

Xiaoping S., (2001). “Vibration and bending of antisymmetrically angle-ply laminated plates with perfectly and weakly bonded layers.” *Composite Struct.,* 53, pp.245-255.

Whitney, J. M. and Pagano, N. J. (1970). “Shear deformation in heterogeneous anisotropic plates.” *ASME J. App. Mech.,* 37, pp.1031-1036.

Wu, Z., Chen, W., and Ren, X. (2010). “An accurate higher-order theory and C0 finite element for free vibration analysis of laminated composite and sandwich plates.” *Composite Struct.,* 92, pp.1299-1307.